

Surprising loss of three-dimensionality in low-energy spin correlations on approaching superconductivity in $\text{Fe}_{1+y}\text{Te}_{1-x}\text{Se}_x$

Zhijun Xu,^{1,2,3,4,5} J. A. Schneeloch,^{1,6} Jinsheng Wen,^{4,5,7} B. L. Winn,⁸ G. E. Granroth,^{8,9} Yang Zhao,^{2,3} Genda Gu,¹ Igor Zaliznyak,¹ J. M. Tranquada,¹ R. J. Birgeneau,^{4,5} and Guangyong Xu^{1,2}

¹*Condensed Matter Physics and Materials Science Department, Brookhaven National Laboratory, Upton, New York 11973, USA*

²*NIST Center for Neutron Research, National Institute of Standards and Technology, Gaithersburg, Maryland 20877*

³*Department of Materials Science and Engineering, University of Maryland, College Park, Maryland, 20742, USA*

⁴*Physics Department, University of California, Berkeley, California 94720, USA*

⁵*Materials Science Division, Lawrence Berkeley National Laboratory, Berkeley, California 94720, USA*

⁶*Department of Physics, Stony Brook University, Stony Brook, New York 11794, USA*

⁷*National Laboratory of Solid State Microstructures and Department of Physics, Nanjing University, Nanjing 210093, China*

⁸*Quantum Condensed Matter Division, Oak Ridge National Laboratory, Oak Ridge, Tennessee 37831, USA*

⁹*Neutron Data Analysis and Visualization Division, Oak Ridge National Laboratory, Oak Ridge, Tennessee 37831, USA*

(Received 4 May 2017; revised manuscript received 19 September 2017; published 6 October 2017)

We report inelastic neutron scattering measurements of low-energy ($\hbar\omega \lesssim 10$ meV) magnetic excitations in the “11” system $\text{Fe}_{1+y}\text{Te}_{1-x}\text{Se}_x$. The spin correlations are two-dimensional (2D) in the superconducting samples at low temperature, but appear much more three-dimensional (3D) when the temperature rises well above $T_c \sim 15$ K, with a clear increase of the (dynamic) spin correlation length perpendicular to the Fe planes. This behavior is extremely unusual; typically, the suppression of thermal fluctuations at low temperature would favor the enhancement of 3D correlations, or even ordering, and the reversion to 2D cannot be naturally explained when only the spin degree of freedom is considered. Our results suggest that the low temperature physics in the 11 system, in particular the evolution of low-energy spin excitations towards superconducting pairing, intrinsically involves changes in orbital correlations.

DOI: [10.1103/PhysRevB.96.134505](https://doi.org/10.1103/PhysRevB.96.134505)

Fe-based superconductors [1–4] (FBS) share many similarities with the high- T_c cuprate family, one of which being that, in general, both systems have parent compounds with long-range antiferromagnetic (AFM) order. When the AFM order is gradually suppressed by doping, superconductivity emerges. The surviving magnetic excitations are widely believed to play vital roles in mediating electron pairing required for superconductivity [5,6]. While the magnetic order in the parent compounds of both FBS and high- T_c cuprates are always three-dimensional (3D), magnetic excitations in their superconducting (SC) derivatives are, however, in general more two-dimensional (2D) in character [7–10]. The spin excitations depend only weakly on momentum transfer perpendicular to the Fe/Cu planes. The interplanar spin correlations are significantly weaker than the in-plane correlations, suggesting the importance of reduced dimensionality for the pairing mechanism in these unconventional superconductors.

On the other hand, unlike high- T_c cuprates where only the Cu $d_{x^2-y^2}$ orbital contributes to bands near the Fermi energy, in FBS, Fe d_{xz} , d_{yz} and d_{xy} orbitals all have significant contributions. The multiorbital nature of the FBS leads to a plethora of new physics. Most notably, electronic nematicity has first been found to develop in the BaFe_2As_2 (122) system [11–16], and then in other FBS as well [17–19]. It is commonly accompanied by (i) splitting of the d_{xz} and d_{yz} orbitals, (ii) magnetic order that breaks the C_4 rotational symmetry, and (iii) lowering of lattice symmetry from C_4 to C_2 . Yet there are situations when not all these features are present. For instance, recent work on the Fe-chalcogenide superconductor (“11” compound) FeSe shows that both lattice and orbital symmetry breaking occur at low temperature [18], while spin correlations remain dynamic [20,21]. The lack of

magnetic order in FeSe has not prevented attempts to describe the system in terms of spin-only models [22,23].

Close to optimal doping in the SC 11 compound $\text{FeTe}_{1-x}\text{Se}_x$, there is no structural transition or magnetic ordering that breaks the C_4 symmetry. Nevertheless, lifting of the degeneracy of the d_{xz} - and d_{yz} -derived electronic bands due to spin-orbit coupling has been observed [19], which is consistent with the lowering of C_4 symmetry of the local hybridization pattern down to C_2 in the presence of stripe-type (0.5,0.5) dynamic short-range magnetic correlations detected by neutron scattering [24,25]. The nematic susceptibility is also found to diverge at low temperature [26]. It appears, therefore, that changes in the orbital and spin correlations may be behind various features observed in the FBS at low temperature, including nematicity. Understanding which one is the fundamental driving force is central to the debate over the SC mechanism [27].

In this paper, we report inelastic neutron scattering measurements of low-energy ($\lesssim 10$ meV) magnetic excitations from a series of $\text{FeTe}_{1-x}\text{Se}_x$ samples. Since they appear to be relevant to both SC and nematicity, the behavior of low-energy spin fluctuations in FBS is of considerable interest. We show that, in the SC samples, upon heating, in addition to the change of in-plane spin correlations from stripe AFM $\mathbf{Q}_{\text{SAF}} = (0.5, 0.5)$ to bicollinear double-stripe AFM $\mathbf{Q}_{\text{DSAF}} = (0.5, 0)$ as reported before [25], the development of the interplanar spin correlations for low-energy spin fluctuations also becomes apparent. Specifically, the low temperature state with stripe AFM in-plane correlations is virtually 2D, with very weak correlations perpendicular to the Fe planes. The high temperature state, however, shows clear correlations between the Fe planes for slowly fluctuating spins, with the interplanar

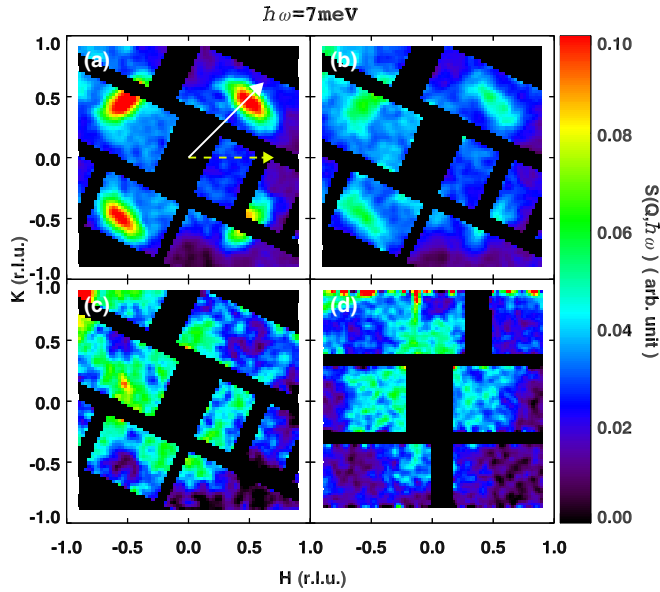


FIG. 1. Inelastic neutron scattering measurements in the $(HK0)$ plane measured on SEQUOIA at energy transfers $\hbar\omega = 7$ meV from (a)–(c) SC40 and (d) Ni10 samples. The samples temperatures are (a) 5 K, (b) 20 K, (c) 200 K, and (d) 5 K. All slices were taken with an energy width of 2 meV. Intensity scale is the same in (a) to (c); data in (d) have been scaled to be directly comparable. Black regions of each panel represent gaps in the detector array.

dynamic correlation length approaching the intraplanar one. Similar effects can also be achieved by changing the chemical composition toward nonsuperconducting (NSC) phases. While it is common to observe 2D magnetic correlations at high temperature that evolve into 3D correlations (or order) at low T , we do not know of any examples of the converse. This highly unusual crossover from a 3D-type spin-liquid at high T to a 2D-type spin-liquid state at low T cannot be explained with effective spin-only models; it is likely due to the change of hybridizations between the Fe d_{xz} , d_{yz} , and d_{xy} orbitals, which implies that the low temperature physics in the 11 material is orbitally driven.

The single crystal $\text{Fe}_{1-z}(\text{Ni})_z\text{Te}_{1-x}\text{Se}_x$ samples used in this experiment were grown by a unidirectional solidification method [28] at Brookhaven National Laboratory. Two SC samples were used, one with optimal doping, $\text{FeTe}_{0.6}\text{Se}_{0.4}$ (SC40) with $T_c \sim 14$ K, and another with 2% Ni doping, $\text{Fe}_{0.98}(\text{Ni})_{0.02}\text{Te}_{0.55}\text{Se}_{0.45}$ (Ni02) with $T_c = 8$ K. The two NSC samples used in these measurements are $\text{Fe}_{1.1}\text{Te}_{0.3}\text{Se}_{0.7}$ (NSC70) and $\text{Fe}_{0.9}(\text{Ni})_{0.1}\text{Te}_{0.55}\text{Se}_{0.45}$ (Ni10). The neutron scattering experiments¹ were performed on the time-of-flight instruments SEQUOIA (BL-17) [29] and

HYSPEC (BL-14B) [30] at the Spallation Neutron Source and Oak Ridge National Laboratory (ORNL), and the BT7 triple-axis-spectrometer at the NIST Center for Neutron Research.

Low-energy magnetic excitations ($\hbar\omega = 7$ meV) in the $(HK0)$ plane from the SC40 and Ni10 samples are shown in Fig. 1. Here the data are integrated along the out-of-plane direction. One can see that in the SC40 sample, the low-energy magnetic excitations appear around $(0.5, 0.5)$ in-plane wave vector for $T \sim T_c$, and there is a clear enhancement of the intensity due to the spin resonance for $T < T_c$. As discussed in previous work [25,31], the low energy spectral weight from SC 11 samples shifts from \mathbf{Q}_{SAF} to \mathbf{Q}_{DSAF} in-plane wave vector upon heating, reflecting a change of in-plane low-energy spin correlations from the “stripe” type to the “double stripe/bicollinear” type. This behavior is observed in SC40 as well when the temperature is raised significantly above T_c [Fig. 1(c)]. The same measurements from NSC samples show that the low-energy spin excitations are always around $\mathbf{Q}_{\text{DSAF}} = (0.5, 0)$ [32] with little variation with T [Fig. 1(d)].

To probe the out-of-plane spin correlations, we measured the L dependence of the magnetic scattering intensities. We first performed measurements in the (HHL) plane, mainly for low energies along $[110]$ from the low temperature stripe-type correlations, marked as the solid arrow in Fig. 1(a). In Fig. 2, we show the intensities at $\hbar\omega = 6.5$ meV. This is the energy where the spin-resonance occurs in optimally doped 11 SC samples, and also where the change of spectral weight with temperature or doping is most pronounced. In Fig. 2(a), we see that the magnetic scattering intensity forms a narrow vertical stripe along the L direction around $(H, H) = (0.5, 0.5)$. The breadth of the intensity along the L direction indicates that the real-space correlations along the c axis are weak. When the sample is heated slightly above T_c to $T = 20$ K, the extra intensity from the spin-resonance disappears, but the shape of the low-energy spectral weight is still defined by the vertical stripe along L [Fig. 2(c)]. Linear cuts along $(0.5, 0.5, L)$ are plotted in Figs. 2(b) and 2(d); here we see that the L dependence of the intensities near \mathbf{Q}_{SAF} at low temperatures is well described by the Fe^{2+} magnetic form factor, suggesting strongly 2D behavior, consistent with previous reports on 11 SC samples [33]. It has been observed in other FBS that the spin-resonance could have 3D dispersions [34]. In our case, note that the 2D spin correlation is present not only for the “spin-resonance” intensity, but also for the low-energy spin excitations in the normal state for T not far above T_c . When heated further to 100 K and 300 K, the stripe-type correlations are destroyed and the intensity near \mathbf{Q}_{SAF} is entirely suppressed [Figs. 2(e)–2(h)]. Similarly, no

¹We use the unit cell that contains two iron atoms. The lattice constants are $a = b \approx 3.8$ Å, and $c \approx 6$ Å. The data are described in reciprocal lattice units (r.l.u.) of $(a^*, b^*, c^*) = (2\pi/a, 2\pi/b, 2\pi/c)$. The measurements in the $(HK0)$ plane were taken on SEQUOIA with the incident neutron beam along the sample $[001]$, $E_i = 50$ meV, and a chopper frequency of 360 Hz. For the measurements in the (HHL) and (HOL) planes taken on HYSPEC, the samples were mounted with $[1\bar{1}0]$ and $[010]$ vertically, respectively, perpendicular to the

horizontal scattering plane. During the HYSPEC measurements, the in-plane orientation of the sample was rotated to cover a range of 180° with 2° step. The data were measured with $E_i = 20$ meV and a chopper frequency of 180 Hz. The area detectors of HYSPEC covered neutrons with scattering angles from 5° to 65° . From the combined data, the constant $\hbar\omega$ slices and linear scans have been symmetrized. Measurements on BT7 were performed with final energy of 14.7 meV, collimations of open- 80° - 80° - 120° and a PG filter after the sample.

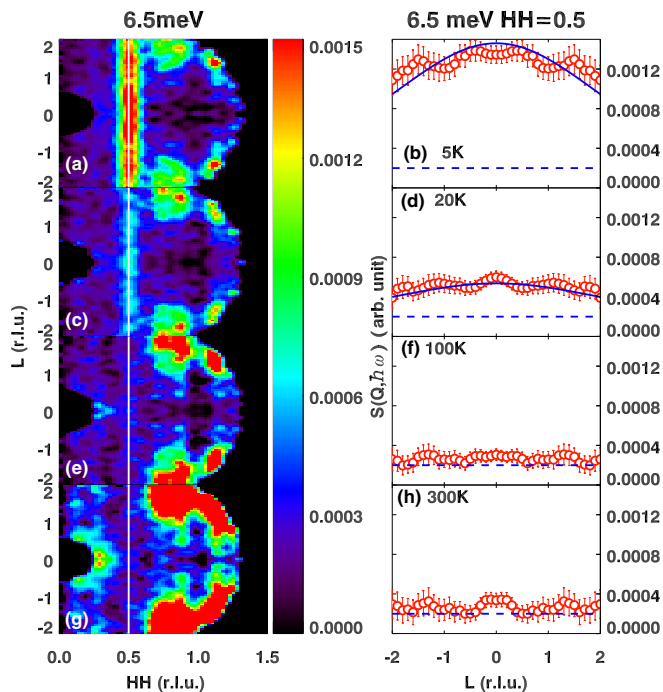


FIG. 2. Inelastic neutron scattering intensity in the (HHL) plane measured on HYSPEC at energy transfer $\hbar\omega = 6.5$ meV from the SC40 sample. Left column are 2D intensity slices, and right column are linear cuts along $(0.5, 0.5, L)$, obtained at (a) and (b): 5 K; (c) and (d) 20 K; (e) and (f) 100 K; and (g) and (h) 300 K. The q -width of the linear cuts is 0.05 r.l.u. along $[110]$ direction. The white line along $(0.5, 0.5, L)$ in the left panels shows where the L cuts in the right column were taken. The dashed lines in right panels are the estimated background obtained from fitting around $(0.65, 0.65, 0)$. The blue solid lines in (b) and (d) are magnetic form factors for a Fe^{2+} ion scaled to the data average. All slices were taken with an energy width of 2 meV. The error bars represent statistical error.

magnetic scattering is observed along $(0.5, 0.5, L)$ from NSC samples (not shown) for all temperatures measured.

In the NSC samples, or in SC samples but at temperatures significantly higher than T_c , the low-energy magnetic spectral weight shifts to $\mathbf{Q}_{\text{D}^{\text{SAF}}}$ corresponding to the bicollinear-type in-plane spin correlations. Measurements along $[100]$ in the (HOL) plane [marked as the dashed arrow in Fig. 1(a)] are plotted in Fig. 3. Here, we show 2D slices and linear cuts at $\hbar\omega = 4$ meV. The reason for this choice of energy transfer is to avoid possible contamination from an anomalous phonon mode [35] that comes in around $(0.5, 0, 0)$ for energies around 7 to 8 meV. Measurements from the Ni10 sample are plotted in Figs. 3(e)–3(h), at $T = 5$ K and 300 K. The L dependence for the low-energy magnetic scattering from the NSC sample is best described by two peaks around $L = \pm 0.5$ r.l.u., suggesting an AFM-type correlation between two adjacent Fe planes.² The intensity from the NSC sample does not change much from 5 K to 300 K, which is expected in a liquidlike phase with strong spin-correlations.

²Note that a modified magnetic form factor, with a faster fall off, is necessary to explain the absence of intensity at $L = \pm 1.5$; see [24].

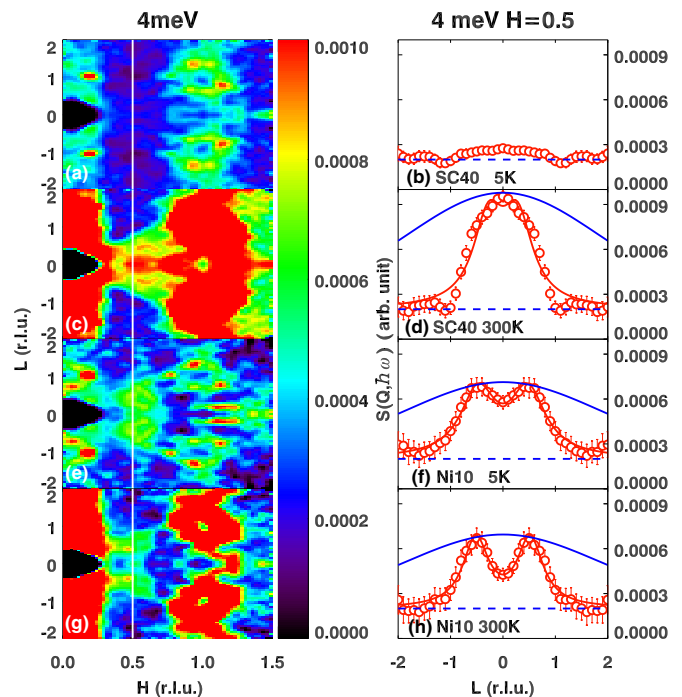


FIG. 3. Inelastic neutron scattering intensities in the (HOL) plane measured on HYSPEC at energy transfer $\hbar\omega = 4$ meV on the SC40 and Ni10 samples. The intensities are scaled by the sample mass for better comparison. Left column are 2D intensity slices, and right column are linear intensity cuts along $(0.5, 0, L)$. The q width of the linear cuts is 0.05 r.l.u. along $[100]$ direction. The panels are (a) and (b): SC40 at 5 K; (c) and (d) SC40 at 300 K; (e) and (f) Ni10 at 5 K; and (g) and (h) Ni10 at 300 K. The white line in the left panels at $H = 0.5$ shows where the L cuts in the right column were taken. The dashed lines in right panels are estimated background values obtained from fitting around $(0.65, 0, 0)$. The blue solid lines in (d), (f), and (h) are magnetic form factors for a Fe^{2+} ion scaled to the data range, and the red solid lines are fits to the data using two symmetric Lorentzians peaked at $L = \pm 0.5$. All slices were taken with an energy width of 2 meV. The error bars represent statistical error.

For the SC40 sample, at base temperature ($T = 5$ K), there is no magnetic scattering intensity near $\mathbf{Q}_{\text{D}^{\text{SAF}}}$ [see Figs. 3(a) and 3(b)], as expected. The development of spectral weight near $\mathbf{Q}_{\text{D}^{\text{SAF}}}$ in SC40 only becomes apparent when the temperature is well above T_c . Data measured at 300 K are shown in Figs. 3(c) and 3(d). In contrast to the stripe-shape intensity distributed broadly along the L direction in the (HHL) plane at low temperature, at high temperature the magnetic scattering in the (HOL) plane has a much narrower span along L [Fig. 3(c)], similar to the data from the NSC sample. The linear cut along $(0.5, 0, L)$ in Fig. 3(d) indicates that the intensity profile decreases much faster with L than what would be expected from the magnetic form factor alone. Compared to the results from the NSC sample, one can still fit the SC40 data with two symmetric peaks [the red line in Fig. 3(d)] but there appears to be more intensity near $L = 0$ from the SC sample instead, suggesting some possible FM component of spin correlations between Fe planes. If we fit the data with Lorentzian functions along L and H directions, we can obtain the dynamic correlation lengths for slowly fluctuating spins along different directions. For

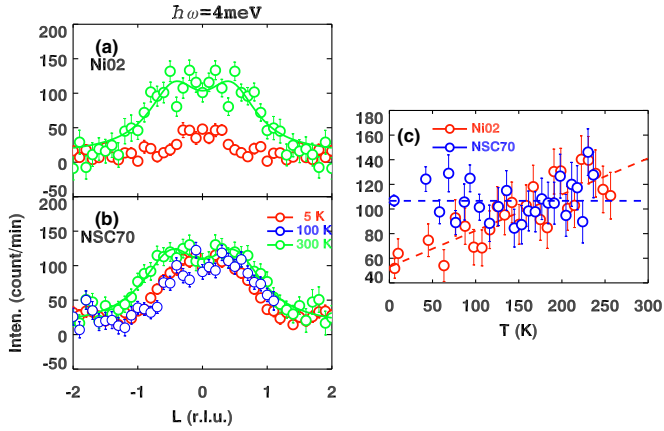


FIG. 4. Inelastic neutron scattering measurements on (a) NiO2 and (b) NSC70 samples along $(0.5, 0, L)$ at energy transfer $\hbar\omega = 4$ meV, performed on BT7. The solid lines are fits to the two symmetric Lorentzian peaked at $L = \pm 0.5$. The intensities at $(0.5, 0, 0.5)$ vs. T for both samples are plotted in (c). The dashed lines are guides to the eye. The error bars represent statistical error.

the Ni10 sample, $\xi_c \sim 1.6(4)$ Å and $\xi_{ab} \sim 2.2(4)$ Å; for the SC40 sample, $\xi_c \sim 1.4(3)$ Å (with fits to two symmetric peaks at $L = \pm 0.5$), and $\xi_{ab} \sim 1.7(4)$ Å. Compared to the situation at low temperature, there is a dramatic enhancement of the interplanar spin correlation in the SC sample, with the interplanar correlation length close to the in-plane one. These results demonstrate that the low-energy magnetic excitations near \mathbf{Q}_{DSAF} , either from the high-temperature phase in the SC sample or from the NSC sample at all temperatures, appear 3D in nature.

Measurements on 11 samples with other compositions not too close to either end (FeTe or FeSe) of the phase diagram [Figs. 4(a) and 4(b)] confirm this trend for slowly fluctuating spins with energy scales of a few meV—3D-like correlations appear in NSC samples at all temperatures, or in SC samples at high temperature, while 2D correlations appear in SC samples at low temperature (temperatures lower than or comparable to T_c). The strength of the 3D spin correlations gradually diminishes with cooling in the SC sample [Fig. 4(c)], yet, in the NSC sample, the spin correlations remain 3D for the entire temperature range (5 K to 300 K) measured.

Many, if not all of these NSC 11 samples already exhibit 3D short-range magnetic order characterized by $\mathbf{Q} \approx (0.5, 0, 0.5)$ at low temperature [36]. It is much more of a puzzle for the 3D spin correlation to become established at high temperature in SC 11 samples and then change to 2D upon cooling. The temperature scale for the 3D to 2D transformation is significantly higher than T_c , suggesting that it is at least not directly tied to the SC phase transition. Also, no explicit magnetic phase transition occurs in this temperature range, nor does the change of the lattice structure favor such an enhancement of the interplanar correlations—the a/c ratio actually decreases at higher temperature in SC 11 samples [25]. Since thermal fluctuations apparently work against such a trend, it is difficult if not impossible to interpret such a spontaneous transformation as driven by spin interactions that can be modeled with a spin-only model. With orbital correlations being the other important degree of freedom in FBS systems,

we look for possible explanations from the change of the different Fe 3d orbitals. ARPES measurements [37] on a SC 11 sample show that, in addition to the lifting of degeneracy between d_{xz} and d_{yz} orbitals at low temperatures due to the spin-orbit coupling, a strong renormalization of the d_{xy} orbital is observed, where the d_{xy} orbital spectral weight decreases at higher temperature, indicative of an orbital selective Mott transition (OSMT) [38–40]. When the d_{xy} orbital delocalizes upon cooling, it can hybridize and interact strongly with the d_{xz} and d_{yz} orbitals. These interactions can create a tendency for an instability that may break the C_4 symmetry at low temperature [41], thus explaining the reported growth in nematic susceptibility [26]. Our results confirm that spin correlations are also significantly affected by this OSMT—when the d_{xy} electrons become less itinerant and carry more local moment at high temperatures, an enhancement of the interplanar spin correlations is observed in the low-energy spin channel. This behavior is reminiscent of the orbital selective electronic localization at high temperature that was first observed in the 11 parent material FeTe [24,42]. In other words, while changes in both orbital and spin channels occur in the same temperature range, the change of spin correlations is likely a result of changing orbital correlations.

Although no electronic nematic order is present in our samples at low temperature, the 2D low-energy spin excitations around $(0.5, 0, 0.5)$ are directly related to nematicity observed in both FeSe [21] and other FBS systems [16]. It is also noteworthy that in the 11 system, as well as in many other FBS, the Fermi surface at low temperature typically forms 2D cylinders at Γ and X points [43,44]. In the 11 system we found that the low-energy magnetic excitations at high temperatures appear highly 3D and are located around in-plane wave-vector $\mathbf{Q}_{\text{DSAF}} = (0.5, 0)$. If they are indeed the bosons that mediate SC pairing at low temperature, these excitations apparently need to become quasi-2D and appear near in-plane wave-vector $\mathbf{Q}_{\text{SAF}} = (0.5, 0.5)$ to satisfy the nesting conditions. With the scenario discussed above, a change in the orbital hybridization is therefore essential for this evolution to quasi-2D spin correlations to occur before superconductivity can set in. Such doping and temperature dependent changes of the orbital hybridization pattern have been recently proposed in the context of the evolution of the in-plane correlations [24]. Our results thus strongly support the idea that both nematicity and superconductivity in the 11 system appear to be fundamentally orbital-driven. This conclusion clearly has significance not just for the 11 system but for all other FBS as well.

The work at Brookhaven National Laboratory was supported by the Office of Basic Energy Sciences, U.S. Department of Energy, under Contract No. DE-SC0012704. Z.J.X. and R.J.B. are also supported by the Office of Science, Basic Energy Sciences, U.S. Department of Energy through Contract No. DE-AC02-05CH11231. The work at ORNL was supported by the U.S. Department of Energy, Office of Science, Office of Basic Energy Sciences, under Contract No. DE-AC05-00OR22725. A portion of this research used resources at the Spallation Neutron Source, a DOE Office of Science user facility operated by the Oak Ridge National Laboratory. The work at Nanjing University was supported by NSFC No. 11374143 and No. 11674157.

- [1] I. I. Mazin, *Nature* **464**, 183 (2010).
- [2] J. Paglione and R. L. Greene, *Nat. Phys.* **6**, 645 (2010).
- [3] J. M. Tranquada, G. Xu, and I. A. Zaliznyak, *J. Magn. Magn. Mater.* **350**, 148 (2014).
- [4] P. D. Johnson, G. Xu, and W.-G. Yin (eds.), *Iron-Based Superconductivity*, Springer Series in Materials Science, Vol. 211 (Springer, Cham, Switzerland, 2015).
- [5] D. J. Scalapino, *Rev. Mod. Phys.* **84**, 1383 (2012).
- [6] P. Dai, *Rev. Mod. Phys.* **87**, 855 (2015).
- [7] S. M. Hayden, G. Aeppli, R. Osborn, A. D. Taylor, T. G. Perring, S. W. Cheong, and Z. Fisk, *Phys. Rev. Lett.* **67**, 3622 (1991).
- [8] S. M. Hayden, G. Aeppli, T. G. Perring, H. A. Mook, and F. Doğan, *Phys. Rev. B* **54**, R6905(R) (1996).
- [9] M. D. Lumsden, A. D. Christianson, D. Parshall, M. B. Stone, S. E. Nagler, G. J. MacDougall, H. A. Mook, K. Lokshin, T. Egami, D. L. Abernathy, E. A. Goremychkin, R. Osborn, M. A. McGuire, A. S. Sefat, R. Jin, B. C. Sales, and D. Mandrus, *Phys. Rev. Lett.* **102**, 107005 (2009).
- [10] M. Ramazanoglu, J. Lamsal, G. S. Tucker, J. Q. Yan, S. Calder, T. Guidi, T. Perring, R. W. McCallum, T. A. Lograsso, A. Kreyssig, A. I. Goldman, and R. J. McQueeney, *Phys. Rev. B* **87**, 140509 (2013).
- [11] J.-H. Chu, J. G. Analytis, K. De Greve, P. L. McMahon, Z. Islam, Y. Yamamoto, and I. R. Fisher, *Science* **329**, 824 (2010).
- [12] M. Yi, D. Lu, J.-H. Chu, J. G. Analytis, A. P. Sorini, A. F. Kemper, B. Moritz, S.-K. Mo, R. G. Moore, M. Hashimoto, W.-S. Lee, Z. Hussain, T. P. Devereaux, I. R. Fisher, and Z.-X. Shen, *Proc. Natl. Acad. Sci. U.S.A.* **108**, 6878 (2011).
- [13] J.-H. Chu, H.-H. Kuo, J. G. Analytis, and I. R. Fisher, *Science* **337**, 710 (2012).
- [14] H.-H. Kuo, M. C. Shapiro, S. C. Riggs, and I. R. Fisher, *Phys. Rev. B* **88**, 085113 (2013).
- [15] M. C. Shapiro, P. Hlobil, A. T. Hristov, A. V. Maharaj, and I. R. Fisher, *Phys. Rev. B* **92**, 235147 (2015).
- [16] X. Lu, J. T. Park, R. Zhang, H. Luo, A. H. Nevidomskyy, Q. Si, and P. Dai, *Science* **345**, 657 (2014).
- [17] E. P. Rosenthal, E. F. Andrade, C. J. Arguello, R. M. Fernandes, L. Y. Xing, X. C. Wang, C. Q. Jin, A. J. Millis, and A. N. Pasupathy, *Nat. Phys.* **10**, 225 (2014).
- [18] S.-H. Baek, D. V. Efremov, J. M. Ok, J. S. Kim, J. van den Brink, and B. Büchner, *Nat. Mater.* **14**, 210 (2015).
- [19] P. D. Johnson, H.-B. Yang, J. D. Rameau, G. D. Gu, Z.-H. Pan, T. Valla, M. Weinert, and A. V. Fedorov, *Phys. Rev. Lett.* **114**, 167001 (2015).
- [20] Q. Wang, Y. Shen, B. Pan, Y. Hao, M. Ma, F. Zhou, P. Steffens, K. Schmalzl, T. R. Forrest, M. Abdel-Hafez, X. Chen, D. A. Chareev, A. N. Vasiliev, P. Bourges, Y. Sidis, H. Cao, and J. Zhao, *Nat. Mater.* **15**, 159 (2016).
- [21] Q. S. Wang, Y. Shen, B. Y. Pan, X. W. Zhang, K. Ikeuchi, K. Iida, A. D. Christianson, H. C. Walker, D. T. Adroja, M. Abdel-Hafez, X. J. Chen, D. A. Chareev, A. N. Vasiliev, and J. Zhao, *Nature Communications* **7**, 12182 (2016).
- [22] F. Wang, S. A. Kivelson, and D.-H. Lee, *Nat. Phys.* **11**, 959 (2015).
- [23] J. K. Glasbrenner, I. I. Mazin, H. O. Jeschke, P. J. Hirschfeld, R. M. Fernandes, and R. Valenti, *Nat. Phys.* **11**, 953 (2015).
- [24] I. Zaliznyak, A. T. Savici, M. Lumsden, A. Tselik, R. Hu, and C. Petrovic, *Proc. Natl. Acad. Sci. U.S.A.* **112**, 10316 (2015).
- [25] Z. Xu, J. A. Schneeloch, J. Wen, E. S. Božin, G. E. Granroth, B. L. Winn, M. Feyngenson, R. J. Birgeneau, G. Gu, I. A. Zaliznyak, J. M. Tranquada, and G. Xu, *Phys. Rev. B* **93**, 104517 (2016).
- [26] H.-H. Kuo, J.-H. Chu, J. C. Palmstrom, S. A. Kivelson, and I. R. Fisher, *Science* **352**, 958 (2016).
- [27] R. M. Fernandes, A. V. Chubukov, and J. Schmalian, *Nat. Phys.* **10**, 97 (2014).
- [28] J. Wen, G. Xu, G. Gu, J. M. Tranquada, and R. J. Birgeneau, *Rep. Prog. Phys.* **74**, 124503 (2011).
- [29] G. E. Granroth, A. I. Kolesnikov, T. E. Sherline, J. P. Clancy, K. A. Ross, J. P. C. Ruff, B. D. Gaulin, and S. E. Nagler, *J. Phys. Conf. Ser.* **251**, 012058 (2010).
- [30] B. Winn, U. Filges, V. O. Garlea, M. Graves-Brook, M. Hagen, C. Jiang, M. Kenzelmann, L. Passell, S. M. Shapiro, X. Tong, and I. Zaliznyak, *EPJ Web of Conf.* **83**, 03017 (2015).
- [31] Z. Xu, J. Wen, J. Schneeloch, A. D. Christianson, R. J. Birgeneau, G. Gu, J. M. Tranquada, and G. Xu, *Phys. Rev. B* **89**, 174517 (2014).
- [32] T. J. Liu, J. Hu, B. Qian, D. Fobes, Z. Q. Mao, W. Bao, M. Reehuis, S. A. J. Kimber, K. Prokes, S. Matas, D. N. Argyriou, A. Hiess, A. Rotaru, H. Pham, L. Spinu, Y. Qiu, V. Thampy, A. T. Savici, J. A. Rodriguez, and C. Broholm, *Nat. Mater.* **9**, 718 (2010).
- [33] Y. Qiu, W. Bao, Y. Zhao, C. Broholm, V. Stanev, Z. Tesanovic, Y. C. Gasparovic, S. Chang, J. Hu, B. Qian, M. Fang, and Z. Mao, *Phys. Rev. Lett.* **103**, 067008 (2009).
- [34] S. Chi, A. Schneidewind, J. Zhao, L. W. Harriger, L. Li, Y. Luo, G. Cao, Z. A. Xu, M. Loewenhaupt, J. Hu, and P. Dai, *Phys. Rev. Lett.* **102**, 107006 (2009).
- [35] D. M. Fobes, I. A. Zaliznyak, J. M. Tranquada, Z. Xu, G. Gu, X.-G. He, W. Ku, Y. Zhao, M. Matsuda, V. O. Garlea, and B. Winn, *Phys. Rev. B* **94**, 121103 (2016).
- [36] J. Wen, G. Xu, Z. Xu, Z. W. Lin, Q. Li, W. Ratcliff, G. Gu, and J. M. Tranquada, *Phys. Rev. B* **80**, 104506 (2009).
- [37] M. Yi, Z.-K. Liu, Y. Zhang, R. Yu, J.-X. Zhu, J. J. Lee, R. G. Moore, F. T. Schmitt, W. Li, S. C. Riggs, J.-H. Chu, B. Lv, J. Hu, M. Hashimoto, S.-K. Mo, Z. Hussain, Z. Q. Mao, C. W. Chu, I. R. Fisher, Q. Si, Z.-X. Shen, and D. H. Lu, *Nat. Commun.* **6**, 7777 (2015).
- [38] L. de' Medici, S. R. Hassan, M. Capone, and X. Dai, *Phys. Rev. Lett.* **102**, 126401 (2009).
- [39] H. Lee, Y.-Z. Zhang, H. O. Jeschke, R. Valentí, and H. Monien, *Phys. Rev. Lett.* **104**, 026402 (2010).
- [40] R. Yu and Q. Si, *Phys. Rev. Lett.* **110**, 146402 (2013).
- [41] V. Stanev and P. B. Littlewood, *Phys. Rev. B* **87**, 161122 (2013).
- [42] D. Fobes, I. A. Zaliznyak, Z. J. Xu, R. D. Zhong, G. D. Gu, J. M. Tranquada, L. Harriger, D. Singh, V. O. Garlea, M. Lumsden, and B. Winn, *Phys. Rev. Lett.* **112**, 187202 (2014).
- [43] M. Sunagawa, T. Ishiga, K. Tsubota, T. Jabuchi, J. Sonoyama, K. Iba, K. Kudo, M. Nohara, K. Ono, H. Kumigashira, T. Matsushita, M. Arita, K. Shimada, H. Namatame, M. Taniguchi, T. Wakita, Y. Muraoka, and T. Yokoya, *Sci. Rep.* **4**, 4381 (2014).
- [44] A. Subedi, L. Zhang, D. J. Singh, and M. H. Du, *Phys. Rev. B* **78**, 134514 (2008).